FULL PAPER

Advances in vibrational configuration interaction theory - part 1: Efficient calculation of vibrational angular momentum terms

Tina Mathea | Guntram Rauhut [ID]

Institute for Theoretical Chemistry, University of Stuttgart, Stuttgart, Germany

Correspondence
Guntram Rauhut, Institute for Theoretical Chemistry, University of Stuttgart, Pfaffenwaldring 55, D-70569 Stuttgart, Germany.
Email: rauhut@theochem.uni-stuttgart.de

Abstract

Finite basis vibrational configuration interaction theory (VCI) is a highly accurate method for the variational calculation of state energies and related properties, but suffers from fast growing computational costs in dependence of the size of the correlation space. In this series of papers, concepts and techniques will be presented, which diminish the computational demands and thus broaden the applicability of this method to larger molecules or more complex situations. This first part focuses on a highly efficient implementation of the vibrational angular momentum (VAM) terms as occurring in the Watson Hamiltonian and the prediagonalization of initial subspaces within an iterative configuration selective VCI implementation. Working equations and benchmark calculations are provided, the latter demonstrating the increased performance of the new algorithm.

KEYWORDS

vibrational angular momentum terms, vibrational configuration interaction theory, vibrational structure theory

1 | INTRODUCTION

The variational calculation of accurate vibrational spectra is a demanding task and many routes have been devised to reduce the computational effort of such calculations.[1–13] It is the size of the correlation space, which constitutes the primary bottleneck and which is combated by the concept of configuration selection.[2–5] Different variants of configuration selective vibrational configuration interaction theory, cs-VCI, have been developed, but common to all is a criterion, which allows to decide about the importance of an individual Hartree product. The evaluation of this criterion, which usually involves the determination of many integrals, may again be computationally demanding, in particular for molecules with more than a couple of atoms and in the case that high-order terms within the expansion of the potential energy surface, PES, have been included, for example, 4-mode coupling terms. In order to reduce the overall CPU time of a cs-VCI calculation, the different individual steps of such a calculation have to be optimized. For example, an iterative cs-VCI calculation based on a criterion related to 2nd order vibrational Møller-Plesset perturbation theory, VMP2, or 2x2 VCI matrices relies on three major steps: (1) the evaluation of the selection criterion, (2) the set-up of an intermediate VCI matrix in the subspace of selected configurations, and (3) its diagonalization or, more precisely, the determination of the eigenpair of interest. While we have presented a new and highly efficient residuum based eigenvalue solver, RACE, for interior eigenpairs some years ago,[14] less has been done with respect to an acceleration of the other two aspects—besides the contraction of integrals[15]—which leads to substantial savings for potential energy surfaces with high-order contributions.

In this series of articles, we present new technical aspects of cs-VCI theory, which lead to significant speed-ups and thus allow for the application of cs-VCI theory to even larger molecular systems. Those concepts, which act on the selection criterion, in principle may have impact on the final results, while all others do not. However, in all cases the observed deviations are less than one wavenumber and are thus negligible for most applications and much lower than the intrinsic error bar of the electronic structure method used for spanning the PES. This first paper focuses on the vibrational angular momentum (VAM) terms, whose calculation within building the VCI matrix may require significant computational effort, especially for large systems. Unrolled analytical expressions are presented, which constitute the basis for a fast and efficient evaluation of these terms. For a constant μ-tensor within the Watson Hamiltonian this ends up in substantially reduced computational cost. Subsequently, an alternative set-up of the initial configuration space within the iterative configuration selection and diagonalization of the resulting subspace will be discussed. This improves the convergence behavior of the iterations and leads to an overall stabilization of the algorithm. We will discuss these two aspects independently from each other and thus two subsections being split into a theory part and subsequent benchmarks will be presented below. Both algorithms presented in the following have been implemented into the MOLPRO package of ab initio programs.[16]

2 | VIBRATIONAL ANGULAR MOMENTUM TERMS

In the following, general aspects regarding an implementation of the VAM terms will be outlined, being necessary for an understanding of what follows. The Hamiltonian, which will be employed within this work, is the commonly used Watson Hamiltonian for non-rotating molecules ($J=0$),[17] which is given as

$$H = \frac{1}{2}\sum_{\alpha\beta}\pi_\alpha\mu_{\alpha\beta}\pi_\beta - \frac{1}{8}\sum_\alpha\mu_{\alpha\alpha} - \frac{1}{2}\sum_i\partial^2_{q_i} + V(q_1,...,q_M) \tag{1}$$

with M being the number of modes of the system. The first term describes the VAM terms, the third one denotes the kinetic energy contribution. The second term, the Watson correction term, will be added as a mass-dependent pseudopotential to the potential energy surface (PES), V, for which we use an n-mode expansion.[18,19]

Mainly due to the large computational cost and due to their intricate implementation, the VAM terms are neglected in some works,[20–23] while others take them into account.[7,24,25] Neglecting VAM contributions may be justified, if large molecules and low lying transitions are considered, since the correction obtained decreases with increasing system size. Nevertheless, for highly accurate calculations, energetically high lying states, rather small systems and molecules showing large amplitude motion (especially double well potentials) and rovibrational calculations these terms are indispensable.

The evaluation of the VAM terms might dominate the evaluation of a VCI matrix element. In Equation (1), the VAM operator π_α is given as

$$\pi_\alpha = -i\sum_{kl}\zeta^\alpha_{lk}q_l\partial_{q_k} \tag{2}$$

with rectilinear normal coordinates q_i and the Coriolis-coupling coefficients ζ^α_{lk} fulfilling $\zeta^\alpha_{lk} = -\zeta^\alpha_{kl}$ and $\zeta^\alpha_{kk} = 0$, $\alpha,\beta \in \{x,y,z\}$. The ζ^α_{lk} are given as cross products

$$\zeta^\alpha_{lk} = \sum_a (\mathbf{L}_{al} \times \mathbf{L}_{ak})_\alpha \tag{3}$$

of the unitary matrix of displacement vectors $\mathbf{L}$ transforming mass-weighted displacement coordinates into normal coordinates. The μ-tensor is connected with the moment of inertia tensor I of the molecule via

$$\mu_{\alpha\beta} = \left(I'^{-1}\right)_{\alpha\beta} \tag{4}$$

with

$$I' = I - \sum_{ijk}\zeta^\alpha_{ik}\zeta^\beta_{jk}q_iq_j. \tag{5}$$

In analogy to the expansion of the potential energy surfaces, an n-mode expansion for the μ-tensor surface[25] will be used, which is given as

$$\mu_{\alpha\beta} = \mu^0_{\alpha\beta} + \sum_i\mu_{\alpha\beta}(q_i) + \sum_{i<j}\mu_{\alpha\beta}(q_i,q_j) + \cdots. \tag{6}$$

The matrix element of two Hartree products (configurations) $|\Phi_I\rangle$ and $|\Phi_J\rangle$ and the first term of Equation (1) is thus given as

$$\langle\Phi_I|H_{VAM}|\Phi_J\rangle = -\frac{1}{2}\sum_{\alpha\beta}\sum_{rstu}\zeta^\alpha_{rs}\zeta^\beta_{tu}\left[\mu^0_{\alpha\beta}\langle\Phi_I|q_r\partial_{q_s}q_t\partial_{q_u}|\Phi_J\rangle\right. \tag{7a}$$

$$\left. +\sum_v\langle\Phi_I|q_r\partial_{q_s}\mu_{\alpha\beta}(q_v)q_t\partial_{q_u}|\Phi_J\rangle + ...\right] \tag{7b}$$

Equation (7) clearly shows that the calculation of the matrix elements may be a computationally demanding task since it requires the summation of a relatively large number of elements, which increases with growing dimension of the system. Obviously, for a system with M modes the computational effort for the calculation of these matrix elements restricted to 0D VAM terms scales as $\mathcal{O}(M^4)$ and as $\mathcal{O}(M^5)$ for additionally including 1D terms. Moreover, different operators/integrals have to be used, depending on the running indices referring to the modes $r,s,t,u,...$ in Equation (7), which leads to the use of conditional statements within the implementation.

In previous work[25] the calculation has been speeded up essentially by using a prescreening technique, which only includes contributing index combinations depending on the size of the prefactor $\mu_{\alpha\beta}^0 \zeta_{rs}^\alpha \zeta_{tu}^\beta$, since many of these are very small or do vanish by theory. Of course, this procedure depends on a threshold, but usually one gains at least a factor of about 10 in speed. For further information about this implementation of the VAM terms, we refer to Reference [25], where also details about the calculation of the contributing integrals can be found. Instead of skipping elements by their prefactor, in our new implementation presented here we will focus on the integrals and the structure of Equation (7) in order to remove or at least reduce the dependency on the number of modes. Simplification of Equation (7) by rigorously using symmetry properties and excluding vanishing parts from the summation in advance leads to a substantially smaller computational overhead.

3 | COMPUTATIONAL DETAILS AND BENCHMARK SYSTEMS

In order to prove the reduction of computational effort achieved by the techniques described in the successive sections, we performed extensive benchmark calculations. All calculations presented below have been performed in a fashion close to real applications aiming at highly accurate results, that is, high quality potential energy surfaces (PES) and sufficiently large configuration spaces have been used. Diborane (B_2H_6, D_{2h}), fluoroethane (C_2H_5F, C_s) and allene (C_3H_4, D_{2d}) have been chosen as benchmark systems as these systems display different difficulties within the calculations. For example, the CH-stretchings of fluoroethane show strong resonance/multi-mode character which, inter alia, lead to large configuration spaces. This selection also takes different point groups into account, that is, Abelian versus non-Abelian point groups are considered, which behave differently with respect to the handling of a real-based configuration space (see Reference [26]). This, in addition, allows to consider different situations regarding the exploitation of symmetry properties. B_2H_6, for example, allows for an extensive use of symmetry since it belongs to the point group D_{2h}, whereas for C_2H_5F there is just one symmetry element, which is reflected in larger CPU times.

As mentioned above, in all calculations presented in this work, we used high quality potential energy surfaces spanned by rectilinear normal coordinates, which have been obtained from explicitly correlated coupled-cluster calculations with a basis set of triple-ζ quality, that is, CCSD(T)-F12a/cc-pVTZ-F12. The respective equilibrium geometries have been used as an expansion point for the PES, for which an n-mode expansion,[18,19] being truncated after 4-mode coupling terms, has been employed. In order to restrict the computational effort, a multi-level scheme[27–29] has been utilized. For further details regarding the calculation of the potential energy surfaces, we refer to the original literature, that is, Reference [30] (B_2H_6), Reference [31] (C_3H_4) and Reference [32] (C_2H_5F). A highly efficient Kronecker product fitting procedure[33] has been employed in order to obtain a polynomial representation of the PES. By solving the vibrational self-consistent field (VSCF) equations in a basis of 20 distributed (mode-dependent) Gauss functions,[34–36] we obtain real one-mode wavefunctions (called VSCF modals in the following). These VSCF modals are used to form Hartree products (configurations) that are employed as basis functions to span the correlation space for the VCI calculations. The n_ith modal for coordinate q_i will be denoted $\varphi_i^{n_i}$ in the following, and the respective configurations by $|\Phi_I\rangle = |\prod_i \varphi_i^{n_i}\rangle$. As described above the μ-tensor is expressed in an n-mode expansion as given in Equation (6). In all calculations, the VAM terms are considered (at least) until zeroth order.

For the subsequent VCI calculations, an iterative procedure has been used (Note: For additional and detailed information concerning our VCI algorithm, we refer to References [2,25,26].). We initially generate a configuration space restricted by (a) the number of modes being excited, (b) the number of excitations for a single mode, and (c) the total number of quanta within the configuration. Subsequently, the initial configuration space is reduced by scanning it via a VMP2-based configuration selection criterion[2,37]

$$\epsilon_{AJ}^{(a+1)} = \frac{\left| \sum_{K \in \{a\}} c_{AK}^{(a)} \langle \Phi_K | H' | \Phi_J \rangle \right|^2}{\epsilon_A^{(a)} - \epsilon_J} \tag{8}$$

with the VCI wavefunction

$$|\Psi_A^{(a)}\rangle = \sum_{K \in \{a\}} c_{AK}^{(a)} |\Phi_K\rangle \tag{9}$$

of state A in the ath iteration step and $c_{AK}^{(a)}$ are the respective coefficients. Within this configuration selection process, the correlation space is iteratively increased by employing Equation (8) until convergence of the state energy is reached. Using the algorithm described in Reference [26], the eigenstate having the largest overlap integral with the multi-dimensional harmonic wavefunction is chosen to be the reference state in Equation (9). In order to determine the intermediate VCI wavefunctions within these iterations, we use an iterative eigenvalue solver based on the RACE-algorithm,[14] which has been shown to outperform the commonly used Jacobi–Davidson algorithm. In order to guarantee that the state of interest is tracked properly during the iterations of configuration selection, physically meaningful startvectors are needed.[26]

4 | CALCULATION OF VIBRATIONAL ANGULAR MOMENTUM TERMS

As mentioned in Section 2, within the calculation of VCI matrix elements the evaluation of the contribution of the VAM terms may be a computational bottleneck. Although a brute force implementation can be very much improved by using prescreening techniques,[25] the additional computational time for including VAM contributions is still significant. Therefore, we present here an even more efficient ansatz based on analytical considerations. The underlying equations are modified in a way that most of the numerous elements resulting in

vanishing contributions are excluded from the onset. Additionally, reordering of the terms and rigorous use of symmetry properties of the integrals lead to very compact equations which can be implemented very efficiently. We will only discuss VAM terms of zeroth and first order, respectively, which have been found to be sufficient for most applications.[24,25] Nevertheless, the basic ideas can be easily transferred to higher order contributions.

Major simplifications of Equation (7) can be achieved by the distinction of cases regarding the involved basis functions (modals) included in the two configurations $|\Phi_I\rangle = |\prod_k \varphi_k^{n_k^I}\rangle$ and $|\Phi_J\rangle = |\prod_k \varphi_k^{n_k^J}\rangle$. By doing so, it becomes possible to exploit symmetry properties, to skip vanishing integrals in advance and to unite terms. Let $M_m(|\Phi_I\rangle, |\Phi_J\rangle) = \{i_1, \ldots, i_m\}$ be the set of mode labels, whose corresponding modes differ by the quantum numbers n_k^I and n_k^J of the respective modals. Moreover, let $|M_m(|\Phi_I\rangle, |\Phi_J\rangle)| = m$, that is, $|\prod_k \varphi_k^{n_k^I}\rangle = |\prod_{k \in \{i_1, \ldots, i_m\}} \varphi_k^{n_k^I}\rangle | \prod_{k \in \{i_1, \ldots, i_m\}} \varphi_k^{n_k^J}\rangle$. In all what follows we request the modals, φ, to be orthogonal. In favor of a shorter notation, we will drop the configurations $|\Phi_I\rangle$, $|\Phi_J\rangle$ for the set M_m as long as the context is obvious. Due to the orthogonality of the modals and the separation of the respective multidimensional integrals into products of one-dimensional integrals it is possible to simplify expression (7) in dependence on m. Obviously, if m is larger than the order of the operator, the corresponding expectation value must vanish. Consequently, for a constant μ-tensor there is a maximum m of 4, while for its 1D-terms $m = 5$ and so on.

In the following, independently of m and the order of the μ-tensor, the properties of the one-dimensional integrals shown in Equations (10) and (11) will be exploited in all cases. For the left and right hand sides showing the same function it is

$$\left\langle \varphi_i^{n_i^I} \middle| \partial_{q_i} \middle| \varphi_i^{n_i^I} \right\rangle = 0 \tag{10a}$$

$$\left\langle \varphi_i^{n_i^I} \middle| \partial_{q_i} q_i \middle| \varphi_i^{n_i^I} \right\rangle = \frac{1}{2} \tag{10b}$$

$$\left\langle \varphi_i^{n_i^I} \middle| q_i \partial_{q_i} \middle| \varphi_i^{n_i^I} \right\rangle = -\frac{1}{2}, \tag{10c}$$

while for different ones it holds

$$\left\langle \varphi_i^{n_i^I} \middle| q_i \partial_{q_i} \middle| \varphi_i^{n_i^J} \right\rangle = \left\langle \varphi_i^{n_i^I} \middle| \partial_{q_i} q_i \middle| \varphi_i^{n_i^J} \right\rangle \tag{11}$$

with φ being real valued and normalized functions.

4.1 | Vibrational angular momentum terms of zeroth order

Depending on the summation indices r, s, t, u referring to the modes, one has to distinguish 10 different cases regarding the operators (or integrals, respectively) involved. These are $\langle q_r \partial_{q_s} q_t \partial_{q_u} \rangle$, $\langle q_r \partial_{q_r} q_t \partial_{q_u} \rangle$, $\langle q_r^2 \partial_{q_s} \partial_{q_u} \rangle$, $\langle q_r \partial_{q_r} q_t \partial_{q_s} \rangle$, $\langle q_r \partial_{q_s} q_s \partial_{q_u} \rangle$, $\langle q_r \partial_{q_s}^2 q_t \rangle$,

$\langle q_r \partial_{q_s} q_t \partial_{q_t} \rangle$, $\langle q_r \partial_{q_r} \partial_{q_s} q_s \rangle$, $\langle q_r \partial_{q_r} q_t \partial_{q_t} \rangle$, and $\langle q_r^2 \partial_{q_s}^2 \rangle$. As mentioned above, we have dropped the configurations in the integrals, that is, we write $\langle q_r \partial_{q_s} q_t \partial_{q_u} \rangle$ instead of $\left\langle \varphi_r^{n_r^I} \middle| q_r \middle| \varphi_r^{n_r^J} \right\rangle \left\langle \varphi_s^{n_s^I} \middle| \partial_{q_s} \middle| \varphi_s^{n_s^J} \right\rangle \left\langle \varphi_t^{n_t^I} \middle| q_t \middle| \varphi_t^{n_t^J} \right\rangle \left\langle \varphi_u^{n_u^I} \middle| \partial_{q_u} \middle| \varphi_u^{n_u^J} \right\rangle \prod_{k \neq \{r,s,t,u\}} \delta_{n_k^I, n_k^J}$.

Since $\zeta_{ii}^{\alpha} = 0$, there is no contribution of integrals of types $\langle q_r \partial_{q_r} q_t \partial_{q_u} \rangle$, $\langle q_r \partial_{q_s} q_t \partial_{q_t} \rangle$ and $\langle q_r \partial_{q_r} q_t \partial_{q_t} \rangle$ in Equation (7a). Giving support to a better readability of the following equations, we introduce the abbreviations

$$A_{ij}^{\pm} = \langle \partial_{q_i} \rangle \langle q_j \rangle \pm \langle q_i \rangle \langle \partial_{q_j} \rangle \tag{12}$$

$$B_{ijk} = \langle q_i^2 \rangle \langle \partial_{q_j} \rangle \langle \partial_{q_k} \rangle \tag{13}$$

$$C_{ijk} = \langle q_i \rangle \left\langle \partial_{q_j}^2 \right\rangle \langle q_k \rangle \tag{14}$$

$$F_{ijk} = \varepsilon_{ijk} B_{ijk} - 2\varepsilon_{ijk} \langle q_i \partial_{q_i} \rangle A_{jk}^{+} + \varepsilon_{ijk} C_{jik} \tag{15}$$

$$G_{ijk} = \langle \partial_{q_i} \rangle A_{jk}^{-}, \tag{16}$$

where ε_{ijk} is the Levi-Civita symbol

$$\varepsilon_{ijk} = \begin{cases} +1, & \text{if } (i,j,k) \text{ is an even permuation of } (1,2,3) \\ -1, & \text{if } (i,j,k) \text{ is an odd permuation of } (1,2,3) \\ 0, & \text{otherwise} \end{cases} \tag{17}$$

with arbitrary mode indices i, j, k.

In the following, we present the working equations for the VAM terms of zeroth order for a molecule in arbitrary orientation. Note, that in the case that the system is oriented along its central principal axis of inertia, the summation $\sum_{\alpha\beta}$ in the following equations can be simplified to $\sum_{\alpha, \alpha=\beta}$, that is, only products including diagonal elements of $\mu_{\alpha\beta}^0$ have to be taken into account.

4.1.1 | Off-diagonal elements with $m = 4$

For sufficiently large configuration spaces (which is the case in almost all applications), $m = 4$ is the most common case and, simultaneously, the one that provides the largest savings in comparison to an implementation based on Equation (7a). We show in the following, that the computational effort for evaluating the VAM contribution of the respective matrix element does no longer scale with the number of modes of the system.

Let $M_4 = \{i_1, i_2, i_3, i_4\}$ with $m = 4$, $|\Phi^I\rangle = |\varphi_{i_1}^{n_{i_1}^I} \varphi_{i_2}^{n_{i_2}^I} \varphi_{i_3}^{n_{i_3}^I} \varphi_{i_4}^{n_{i_4}^I}\rangle |\prod_{k \neq \{i_1, i_2, i_3, i_4\}} \varphi_k^{n_k^I}\rangle$ and $|\Phi^J\rangle = |\varphi_{i_1}^{n_{i_1}^J} \varphi_{i_2}^{n_{i_2}^J} \varphi_{i_3}^{n_{i_3}^J} \varphi_{i_4}^{n_{i_4}^J}\rangle |\prod_{k \neq \{i_1, i_2, i_3, i_4\}} \varphi_k^{n_k^J}\rangle$. Due to the orthogonality of the modals, all integrals with less than four different indices vanish and therefore do not contribute. In addition, the only integral in Equation (7a) having four different mode indices, that is, $\langle q_r \partial_{q_s} q_t \partial_{q_u} \rangle$, is different from zero only in the case $\{r,s,t,u\} \in M_4$. Thus, the only combinations of indices contributing are permutations of M_4, that is, 24 non-zero elements remain. Moreover, the integral

$\langle q_r \partial_{q_s} q_t \partial_{q_u} \rangle$ itself is symmetric regarding commuting r and t and s and u, respectively, that is, $\langle q_r \partial_{q_s} q_t \partial_{q_u} \rangle = \langle q_t \partial_{q_u} q_r \partial_{q_s} \rangle$. Since (a) $\mu^0_{\alpha\beta}$ is independent of the indices concerning the modes and (b) it is $\mu^0_{\alpha\beta} = \mu^0_{\beta\alpha}$ and (c) the summation runs over all α, β, there are pairs of identical summands including the prefactor $\zeta^\alpha_{rs} \zeta^\beta_{tu}$. Summarized, using the abbreviation (12), one obtains

$$\left\langle \Phi_I | H^{(m=4)}_{VAM,0D} | \Phi_J \right\rangle = -\frac{1}{2} \sum_{\alpha\beta} \mu^0_{\alpha\beta} \left[\zeta^\alpha_{i_1 i_2} \zeta^\beta_{i_3 i_4} A^-_{i_4 i_3} A^-_{i_2 i_1} + \zeta^\alpha_{i_1 i_3} \zeta^\beta_{i_2 i_4} A^-_{i_4 i_2} A^-_{i_3 i_1} + \zeta^\alpha_{i_1 i_4} \zeta^\beta_{i_2 i_3} A^-_{i_3 i_2} A^-_{i_4 i_1} \right]$$

(18)

Since all the A^- are independent of α and β, they need to be calculated only once per matrix element. Consequently, the computational effort for a zeroth order VAM contribution with $m = 4$ is very low and additionally independent of the number of modes present in the system. Note, that this result refers to the evaluation of the VAM contribution for a single matrix element.

4.1.2 | Off-diagonal elements with $m = 3$

Let $M_3 = \{i_1, i_2, i_3\}$ with $m = 3$, $|\Phi_I\rangle = |\varphi^{n^I_{i_1}}_{i_1} \varphi^{n^I_{i_2}}_{i_2} \varphi^{n^I_{i_3}}_{i_3}\rangle | \prod_{k \neq \{i_1, i_2, i_3\}} \varphi^{n^I_k}_k\rangle$ and $|\Phi_J\rangle = |\varphi^{n^J_{i_1}}_{i_1} \varphi^{n^J_{i_2}}_{i_2} \varphi^{n^J_{i_3}}_{i_3}\rangle | \prod_{k \neq \{i_1, i_2, i_3\}} \varphi^{n^J_k}_k\rangle$. Due to the orthogonality of modals, integrals with less than three different mode indices do not contribute, that is, $\langle q_r \partial_{q_r} \partial_{q_s} q_s \rangle = 0$ and $\langle q^2_r \partial^2_{q_s} \rangle = 0$. There is one integral with four different indices. The term $\langle q_r \partial_{q_s} q_t \partial_{q_u} \rangle$ is symmetrical concerning an interchange of s and u and/or r and t. The integral will not vanish due to Equation (10a), as long as $\{s, u\} \in \{i_1, i_2, i_3\}$. Thus, there are six possible combinations, each two of them having the same prefactor. Consequently, the contribution of the integral $\langle q_r \partial_{q_s} q_t \partial_{q_u} \rangle$ is given by

$$-\frac{1}{2} \sum_{\alpha\beta} 2 \cdot \sum_{t \neq \{i_1, i_2, i_3\}} \langle q_t \rangle \left[\zeta^\alpha_{i_1 i_2} \zeta^\beta_{t i_3} \langle \partial_{q_{i_3}} \rangle A^-_{i_2 i_3} + \zeta^\alpha_{i_1 i_3} \zeta^\beta_{t i_2} \langle \partial_{q_{i_2}} \rangle A^-_{i_3 i_1} + \zeta^\alpha_{i_2 i_3} \zeta^\beta_{t i_1} \langle \partial_{q_{i_1}} \rangle A^-_{i_3 i_2} \right].$$

(19)

There is also a number of integrals having three different mode indices. For each of them, only elements with $\{r, s, t\} \in \{i_1, i_2, i_3\}$, that is, all permutations of M_3, yield non-zero terms. Additionally, by using Equation (11) and taking advantage of the antisymmetry of the ζ-constants, one obtains, after summation over all indices, identical contributions for the integrals $\langle q_r \partial_{q_r} \partial_{q_s} q_t \rangle$ and $\langle q_r \partial_{q_s} q_s \partial_{q_u} \rangle$. Considering all aspects mentioned, a matrix element with $m = 3$ is given as

$$\left\langle \Phi_I | H^{(m=3)}_{VAM,0D} | \Phi_I \right\rangle = -\sum_{\alpha\beta} \mu^0_{\alpha\beta} \left[\zeta^\alpha_{i_1 i_2} \zeta^\beta_{i_1 i_3} F_{i_1 i_2 i_3} + \zeta^\alpha_{i_1 i_2} \zeta^\beta_{i_2 i_3} F_{i_2 i_1 i_3} + \zeta^\alpha_{i_1 i_3} \zeta^\beta_{i_2 i_3} F_{i_3 i_1 i_2} \right. $$
$$\left. + \sum_{t \neq \{i_1, i_2, i_3\}} \langle q_t \rangle \left(\zeta^\alpha_{i_1 i_2} \zeta^\beta_{t i_3} G_{i_3 i_2 i_1} + \zeta^\alpha_{i_1 i_3} \zeta^\beta_{t i_2} G_{i_2 i_3 i_1} + \zeta^\alpha_{i_2 i_3} \zeta^\beta_{t i_1} G_{i_1 i_3 i_2} \right) \right].$$

(20)

A decisive advantage of Equation (20) regarding computational effort is the pre-calculation of certain quantities due to decoupling of indices. The products of the ζ-constants with $\mu^0_{\alpha\beta}$ only depend on α

and β and are independent of the modes. All factors F and G have to be calculated only once per matrix element. This results in a low number of necessary summations which tremendously reduces the computational effort from $\mathcal{O}(M^4)$ to $\mathcal{O}(M)$.

4.1.3 | Off-diagonal elements with $m = 2$

For this case, there are no major simplifications possible. Thus, we will not discuss this case explicitly.

4.1.4 | Off-diagonal elements with $m = 1$

Let $M_1 = \{i_1\}$ with $m = 1$, that is, $|\Phi_I\rangle = |\varphi^{n^I_{i_1}}_{i_1} \prod_{k \neq i_1} \varphi^{n^I_k}_k\rangle$ and $|\Phi_J\rangle = |\varphi^{n^J_{i_1}}_{i_1} \prod_{k \neq i_1} \varphi^{n^J_k}_k\rangle$. Using Equation (10a) one obtains $\langle q_r \partial_{q_s} q_t \partial_{q_u} \rangle = 0$ and $\langle q^2_r \partial_{q_s} \partial_{q_u} \rangle = 0$. Furthermore, it is

$$\sum_{\alpha\beta} \sum_{rst} \mu^0_{\alpha\beta} \zeta^\alpha_{rs} \zeta^\beta_{tr} \langle q_r \partial_{q_r} \partial_{q_s} q_t \rangle = -\sum_{\alpha\beta} \sum_{rsu} \mu^0_{\alpha\beta} \zeta^\alpha_{rs} \zeta^\beta_{su} \langle q_r \partial_{q_s} q_s \partial_{q_u} \rangle, \quad (21)$$

as solely the integrals $\langle q_r \partial_{q_r} \partial_{q_{i_1}} q_t \rangle$ and $\langle q_r \partial_{q_s} q_s \partial_{q_{i_1}} \rangle$ contribute due to Equation (10a). Considering Equations (11) and (10b) (Equation (10c), respectively) and using the symmetry of $\mu^0_{\alpha\beta}$, summation over α and β yields identical terms with different sign. Additionally, the contribution of the integrals $\langle q_r \partial_{q_r} \partial_{q_s} q_s \rangle$ add up to zero, that is, $\sum_{\alpha\beta} \sum_{rs} \mu^0_{\alpha\beta} \zeta^\alpha_{rs} \zeta^\beta_{sr} \langle q_r \partial_{q_r} \partial_{q_s} q_s \rangle = 0$, since the use of Equation (11) leads to two identical parts with reversed sign canceling each other. Finally, one ends up with

$$\left\langle \Phi_I | H^{(m=1)}_{VAM,0D} | \Phi_J \right\rangle = \frac{1}{2} \sum_{\alpha\beta} \mu^0_{\alpha\beta} \sum_{r \neq i_1} \left[\zeta^\alpha_{r i_1} \zeta^\beta_{r i_1} \left(\langle q^2_r \rangle \langle \partial^2_{q_{i_1}} \rangle + \langle q^2_{i_1} \rangle \langle \partial^2_{q_r} \rangle \right) \right.$$
$$\left. - \sum_{s \neq \{r, i_1\}} \zeta^\alpha_{i_1 s} \langle q_r \rangle \left(2 \zeta^\beta_{rs} \langle q_{i_1} \rangle \langle \partial^2_{q_s} \rangle - \zeta^\beta_{r i_1} \langle q_s \rangle \langle \partial^2_{q_{i_1}} \rangle \right) \right] \quad (22)$$

Equation (22) reduces the computational effort of Equation (7a) to $\mathcal{O}(M^2)$.

4.1.5 | Diagonal elements, $m = 0$

For diagonal elements it is $|\Phi_I\rangle = |\Phi_J\rangle$, that is, $M_0 = \emptyset$ with $m = 0$. Using Equation (10a), one obtains $\langle q_r \partial_{q_s} q_t \partial_{q_u} \rangle = 0$, $\langle q^2_r \partial_{q_s} \partial_{q_u} \rangle = 0$, $\langle q_r \partial_{q_r} \partial_{q_s} q_t \rangle = 0$, and $\langle q_r \partial_{q_s} q_s \partial_{q_u} \rangle = 0$. Therefore, only parts containing the integrals $\langle q_r \partial^2_{q_s} q_t \rangle$, $\langle q_r \partial_{q_r} \partial_{q_s} q_s \rangle$, and $\langle q^2_r \partial^2_{q_s} \rangle$ must be considered in Equation (7a). Consequently, considering $\zeta^\alpha_{ii} = -\zeta^\alpha_{ii}$ and Equations (10b) and (10c) one obtains

$$\left\langle \Phi_I | H^{(m=0)}_{VAM,0D} | \Phi_I \right\rangle = -\frac{1}{2} \sum_{\alpha\beta} \mu^0_{\alpha\beta} \sum_r \sum_{s \neq r} \zeta^\alpha_{rs}$$
$$\left(\zeta^\beta_{rs} \left(\frac{1}{4} + \langle q^2_r \rangle \right) + \sum_{t \neq \{r, s\}} \zeta^\beta_{ts} \langle q_r \rangle \langle \partial^2_{q_s} \rangle \langle q_t \rangle \right) \quad (23)$$

TABLE 1 CPU times in seconds for evaluating the VCI matrix depending on the operator calculated with (i) a former implementation based on prescreening[25] (abbrv. As "Prescr.") and (ii) with the implementation based on the equations given in Section 4 ("This work"), the computational savings are given in percent ("Sav.")

	C_2H_5F			B_2H_6			C_3H_4		
	Prescr.	This work	Sav.	Prescr.	This work	Sav.	Prescr.	This work	Sav.
$H_{VAM(0D)}$	315,024	14,588	95.4	20,368	2780	86.3	59,787	4805	92.0
$H_{VAM(0D)}/H_{w/o\,VAM}$	72.0	3.3		10.5	1.4		22.8	1.8	
$H_{VAM(1D,diag)}$	395,442	17,277	95.6	80,573	3854	95.2	102,245	5966	94.2
$H_{VAM(1D,diag)}/H_{w/o\,VAM}$	90.3	3.9		41.6	2.0		38.6	2.3	
$H_{VAM(1D)}$			91.9			92.0			94.3

Note: Relative CPU times refer to a calculation without the VAM operator. The total CPU times for these calculations are 4377.6 s (C_2H_5F), 1936.9 s (B_2H_6) and 2625.0 s (C_3H_4). For B_2H_6 and C_2H_5F, all fundamental transitions have been calculated, for C_3H_4 additionally the first overtones below 2500 cm^{-1} have been considered. Within the 1D calculations, only the ground state has been determined. All CPU times include also the times resulting from the potential energy surface.

Using Equation (23) instead of Equation (7a) reduces the computational effort regarding the number of modes from $\mathcal{O}(M^4)$ to $\mathcal{O}(M^3)$. Note that, these diagonal elements are the rarest within the evaluation of the VCI matrix.

4.2 | Results

In order to determine the computational savings generated by the ansatz presented above, we performed benchmark calculations for the three test molecules. Although the computational effort for including the VAM contributions is independent of the expansion order of the PES, in all calculations we took couplings up to fourth order into account (see Section 3), which was found to be necessary for accurate results. The initial VCI configuration spaces for the calculations have been chosen as follows: For C_2H_5F we used up to five simultaneously excited modes and a maximal excitation per mode of five. The calculations for B_2H_6 and C_3H_4 have been performed with up to 6 modes excited and a maximum excitation of not more than 6 (7 in case of C_3H_4) per mode. The sum of quantum numbers per configurations has been limited to 15 in all cases. We determined CPU times required for the calculation of all matrix elements needed within the calculation of all fundamental transitions, that is, 19 high quality energies (including the ZPVE) have been evaluated for C_2H_5F and B_2H_6, respectively. For C_3H_4, also the first overtones below 2500 cm^{-1} have been calculated. One set of calculations has been performed by using our former prescreening algorithm as described in Reference [25], the other one with the new ansatz described in Section 4. Timings and savings arising from the new algorithm are summarized in Table 1.

Figure 1 shows the CPU times for building the VCI matrix using the equation shown above (light blue bars) with respect to our former implementation (red bars). In order to visualize the order of the effect, we also ran calculations using a brute force implementation of Equation (7), for example, no optimization by prescreening has been used (orange bars). It is important to notice that all CPU times shown
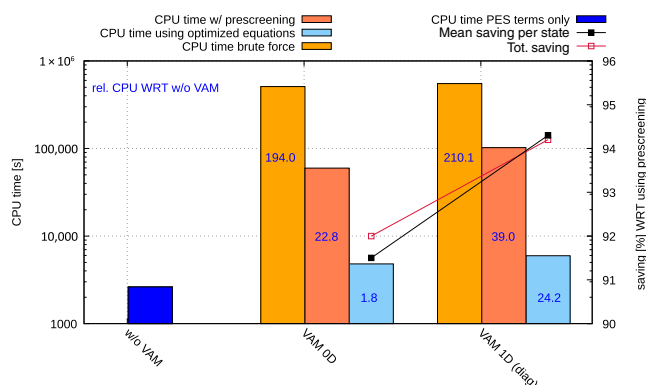

FIGURE 1 Comparison of different implementations (brute force, an implementation based on prescreening[25] and this work based on Equations (18), (20), (22), and (23) (0D) and the equations shown in the Appendix (1D)) regarding CPU times for evaluating the VCI matrix within the calculation depending on the operator included. The times shown refer to the calculation of the fundamentals and first overtones below 2500 cm^{-1}, that is, 19 states are included. Relative CPU times with respect to a calculation excluding the VAM contributions are given in blue, the second y-axis depicts the computational savings with respect to the implementation using prescreening

also include the computational time required for evaluating the PES contributions. Since the configuration spaces for two calculations, one including VAM contributions and the other not, may differ from each other, we compare CPU times including contributions from the PES. In order to provide the magnitude of the CPU time needed for the PES parts, the dark blue bar refers to the calculation without VAM contributions. The blue numbers within the bars show the relative CPU time with respect to a calculation excluding VAM terms. Note, that the y-axis on the left hand side referring to the total CPU time shows a logarithmic scale, while the second y-axis on the right hand side is linear and shows the computational savings relative to the CPU time using the algorithm based on prescreening.

As Figure 1 clearly shows, using Equations (18), (20), (22), and (23) (0D) and the equations from Appendix A (1D) result in tremendous computational savings in CPU time. For allene, including the VAM contributions of 0th order increases the CPU time by a factor 1.8 in CPU time. The mean saving per state is 91.5%, while the total one has a value of 92.0%. The enormous computational saving primarily is generated by the cases $m = 4$ and $m = 3$, since these render the largest reduction regarding the number of elements to be summed up. Also precalculation of certain parts can be exploited in these cases maximally.

On average (based on the data in Table 1), our new implementation relying on the equations presented in Section 4 is approximately 12 times faster than the former one for 0D VAM contributions, 20 times faster for also including 1D VAM contributions for the diagonal elements and 12 times faster for considering 0D and 1D VAM terms for all matrix elements (see Table 1). Compared with the computational effort for calculating the contributions of the potential energy surfaces, including the 0D VAM terms, which include the most important physically relevant contributions and are often sufficient, is no longer a computational bottleneck. Note that, in the following all CPU times given refer to the new implementation.

5 | PREDIAGONALIZATION OF SUBSPACES

States located in regions of high state density often suffer from comparatively slow convergence within iterative configuration selection algorithms, for example, cs-VCI. In the following, we present a method to improve the convergence of vibrational state energies and the VCI wavefunction based on spanning meaningful subspaces of the correlation space and prediagonalize them. In our benchmark calculations, we put a special focus on fundamentals belonging to CH-stretching modes, since these often show rather slow convergence.

5.1 | Method and implementation

As described in Section 3, within our implementation of VCI theory each calculation starts by generating an initial configuration space restricted by (a) the maximum number of modes excited within the configurations ($n_{ex,init.}$), (b) the maximum excitation within one oscillator ($n_{max,init.}$) and (c) the sum of quantum numbers within one Hartree product ($n_{sum,init.}$). Simplest, the starting wavefunction (9) in the initial iteration step of the configuration selective procedure is given by the corresponding VSCF configuration. For Abelian systems and rectilinear normal coordinates, a single Hartree product is used, otherwise meaningful linear combinations representing all physically relevant information are employed, that is,

$$|\Psi_A^{(1)}\rangle = \begin{cases} |\Phi_0\rangle & \text{for Abelian systems} \\ \sum_n c_n |\Phi_n\rangle & \text{else, e.g., non-Abelian systems and/or localized normal coordinates} \end{cases}$$

(24)

with the coefficients c_n describing meaningful linear combinations of real-valued configurations covering additional quantum numbers as, for example, the l-quantum number. For further details, we refer to Reference [26]. Subsequently, Equation (8) is utilized for the configuration selection process. Note that, the whole initial correlation space is screened in this step. After building the VCI matrix in the correlation space of selected configurations, the targeted eigenvalue is determined by an iterative eigenvalue solver employing the harmonic representation of the reference wavefunction of the first iteration step (24) as startvector. Convergence is defined to be reached if the difference of the state energies of two consecutive iterations is below a given threshold. This procedure refers to our former implementation and will be used as reference regarding performance in the following.

In our new ansatz aiming at an improvement of the convergence behavior of critical states regarding the number of necessary iteration steps, we essentially modify two steps within the algorithm described above:

(i) We replace the starting wavefunction (24) by a wavefunction containing static correlation effects. In order to do so, we define a meaningful subspace (abbreviated as "subsp." in what follows) of the initial correlation space, which includes configurations showing resonances with the reference state. In analogy to the notation for the initial configuration space, we denote the characteristic values describing the size of the subspace $n_{ex,subsp.}$, $n_{max,subsp.}$, and $n_{sum,subsp.}$. The set of configurations contained in the subspace, is denoted $K_{tot,subsp.}$. Usually the most important resonances are of Fermi- or Darling-Dennison type. Thus, we choose $n_{ex,subsp.} = 3$ and $n_{max,subsp.} = 3$ with a value of 4 up to 5 for $n_{max,subsp.}$ depending on the size of the initial correlation space (these values refer to the reference configuration $|\Phi_0\rangle$ and not to the ground state configuration). Note, that the subspace is generated exactly as the initial configuration space, that is, not a subspace of modes is used, but the configurations included are chosen via the parameters $n_{ex,subsp.}$, $n_{max,subsp.}$, and $n_{sum,subsp.}$ and regardless of the state of interest all modes are treated equally. In most cases, the values mentioned cover the most contributing resonances, but they may be increased if necessary. Note that, choosing a subspace of configurations is somewhat related to the concept presented in Reference [38], but here additionally resonance effects are addressed explicitly, which leads to a more generalized ansatz.

Subsequently, we prediagonalize the defined subspace and use our state picking scheme to identify the state of interest, that is, the one with the largest overlap with the harmonic reference state. The chosen eigenstate obtained by the diagonalization of the subspace can be written as eigenvector

$$|\Psi_A^{(1)}\rangle = \sum_{I \in K_{tot,subsp.}} c_{AI} |\Phi_I\rangle,$$

(25)

with c_{AI} being the respective coefficients. The state (25) is used instead of (24) within Equation (8) for constructing the correlation space. Note, that we include all the configurations from the chosen subspace in the selected configuration space regardless of their contribution according to Equation (8).

(ii) Instead of using the harmonic representation of the state (24) as starting vector for the iterative eigenvector solver used, we now employ the eigenstate (25) obtained from the prediagonalization of the subspace chosen. Particularly in cases of multi-resonance effects, this leads to more stability within the calculation from the very beginning.

The modifications (i) and (ii) result in manifold effects: At the beginning of the calculation (that is, iteration step one) the actual wavefunction of the state of interest is better described by the expression (25) than by (24) since it contains resonance information, not being contained in a single configuration. Thus, subsequently (in the next iteration step) selected configurations will be more appropriate in order to describe the full wavefunction since important couplings are taken into account from the beginning of the calculation. Consequently, the number of unnecessary configurations, which are "mistakenly" selected due to the unbalanced treatment, decreases. Finally, this may lead to smaller configuration spaces when convergence is reached and the entire calculation gains more stability, in particular for states showing multi-resonance effects.

The effects of the described modifications on the CPU time depends on the system and the state under consideration: On the one hand, the configuration spaces may be smaller during the iterations. In this case, all three major steps within the calculation (that is, matrix set-up, diagonalization and configurations selection) are speeded up. On the other hand, a smaller number of iterations compared to the old algorithm may be necessary, since the selected configuration space of the 1st iteration fits better to the target state. As a consequence, convergence is reached faster by using the prediagonalization of meaningful subspaces. Both effects can occur and also add up, as revealed by our benchmark calculations.

5.2 | Results

In order to prove the prediagonalization of appropriate subspaces leading to faster convergence for states lying in regions of high state density, we performed benchmark calculations based on 4D PESs including 0D VAM terms for the CH and BH-stretching modes of B_2H_6, C_3H_4, and C_2H_5F. The initial configuration space has been restricted by $n_{ex,init.} = 6$, $n_{max,init.} = 6$, and $n_{sum,init.} = 15$ in all cases. For defining the subspace, we used $n_{ex,subsp.} = 3$, $n_{max,subsp.} = 3$, and $n_{sum,subsp.} = 4$ (B_2H_6 and C_2H_5F) and $n_{sum,subsp.} = 5$ (C_3H_4), respectively.

Table 2 lists the CPU time savings and the deviations of the energy eigenvalues with respect to our former implementation without prediagonalizing subspaces. As the data shows, the energies obtained by both methods differ by less than 0.2 cm^{-1} and we obtain a mean deviation of not more than 0.1 cm^{-1} per state which is negligible in comparison to other possible error sources. On the other hand, on average (all three systems considered) 17.1% CPU time per state are saved and 17.3% in total.

In Figure 2, a detailed breakdown of the CPU times needed for the three most time consuming steps within our iterative VCI implementation is shown for allene, which has four CH-stretching modes: ν_1 (A$_1$), ν_5 (B$_2$) and two degenerate states ν_8^{+1} (E) and ν_8^{-1} (E). We label the degenerate states by $\nu_8^{|+1|}$ and $\nu_8^{|-1|}$, because within our real based VCI implementation degenerate states with different l-quantum number are only specified by their absolute value l due to the fact that we consider real linear combinations of configurations in order to represent all physically relevant information present in the complex basis. The bars in Figure 2 provide the CPU time needed for the complete calculation of the given fundamental transitions sorted by time for diagonalization (red), matrix build-up (blue) and configuration selection (orange). The red numbers depict the dimension of the final configuration space. The lines refer to the second y-axis and show the number of iterations needed by the algorithm in order to reach convergence (without (blue) and with (black) prediagonalization).

As can be seen, in all cases the number of required iterations is larger when using our former algorithm not considering subspaces. Of course, omitting whole iteration steps leads to relatively large CPU time savings. On average, 1.3 iterations per state are saved within the calculations for allene, 1.2 for C_2H_5F and 0.0 for B_2H_6. As the configuration selection has the largest share with respect to the total CPU time, it is also responsible for most of the CPU time savings if an iteration can be left out. Note, that we lose performance by directly including *all* configurations from the subspace in the current configuration space without selection via criterion (8). Nevertheless, this loss is essentially overcompensated by saving

	B_2H_6	C_2H_5F	C_3H_4
Mean CPU saving (%) per state	18.8	12.1	20.5
Mean ΔE per state (cm^{-1})	0.0	0.1	0.0
Max. ΔE (cm^{-1})	0.0	0.2	0.1
Tot. CPU saving (%) (all states)	18.5	13.6	19.7

TABLE 2 CPU time savings and energy deviations resulting from employing the prediagonalization of subspaces

Note: For all systems, the fundamentals belonging to the CH-stretching and BH-stretching modes, respectively, have been calculated. We used $n_{ex,init.} = 6$, $n_{max,init.} = 6$, and $n_{sum,init.} = 15$ for the initial correlation space in all cases. For defining the subspace, we employed $n_{ex,subsp.=3}$, $n_{max,subsp.=3}$, and $n_{sum,subsp.} = 4$ (B_2H_6 and C_2H_5F) and $n_{sum,subsp.} = 5$ (C_3H_4), respectively. For details regarding the single states see Tables S1–S3 in the Supporting information.
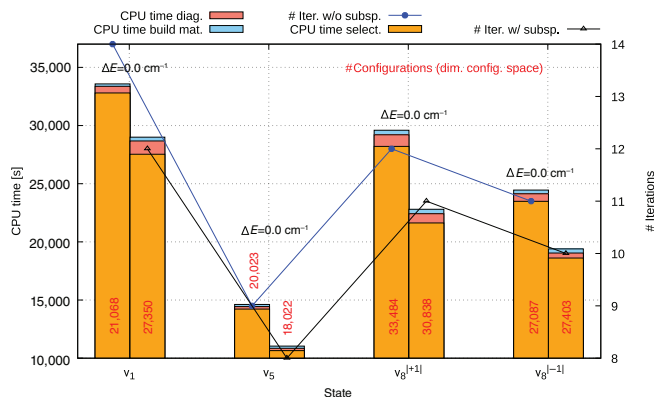
FIGURE 2 CPU times for the calculation of the four CH-stretching modes of C_3H_4, split up in times for building and diagonalizing the VCI matrix and employing the configuration selection scheme based on Equation (8). For every state shown, the bar on the right hand side shows the CPU time of the calculation using the prediagonalization of a meaningful subspace whereas the bar on the left hand side is the reference calculation. The corresponding differences between the resulting energies are given above the bars, the dimensions of the associated correlation spaces are depicted in red. The second y-axis on the RHS shows the number of iterations required

iteration steps. Although we handle larger configuration spaces in comparison to the former implementation at the beginning of the calculation, the computational effort for the last iteration steps is substantially larger. This is mainly due to the rising cost of the selection process and the diagonalization, both dramatically increasing for almost converged (and therefore large) correlation spaces. On the other hand, the dimension of the correlation space is smaller by using the new algorithm for the states ν_5 and $\nu_8^{|+1|}$ of allene, but larger for the two states ν_5 and $\nu_8^{|-1|}$. It can be seen in Figure 2, that the savings for the matrix set-up and its diagonalization due to the smaller correlation spaces are not too large, since the configuration selection dominates the total CPU time in the case of allene (see above). Nevertheless, for the states ν_5 and $\nu_8^{|+1|}$ the smaller dimensions lead to CPU time savings, while most of the extra time using our former algorithm is used for further optimization of the configuration space, that is, configuration selection. In contrast, in the case of B_2H_6 (see Table S1 in the Supporting information), all of the CPU time savings generated by using the concept of subspaces results from smaller correlation spaces. Here, matrix set-up, diagonalization and configuration selection become faster due to smaller correlation spaces during the iterations. The same holds true for C_2H_5F, the final configuration spaces on average are smaller for all states, on average 10,500 configurations are saved (see Table S2 in the Supporting information).

In summary, as demonstrated by the benchmark calculations above, the ansatz of improving the start vector for the configuration selection scheme by considering resonances from the very beginning leads to a faster convergence of the correlation space. Additionally, the number of required iterations decreases in some cases and leads

to CPU time savings. The results for the energy eigenvalues are almost identical, that is, there is no loss of accuracy here.

6 | SUMMARY

Two strategies have been presented for the acceleration of vibrational configuration interaction calculation, the first one being applicable to any VCI implementation, while the 2nd is specific to configuration selective variants. It was found that computational bottlenecks arising from the VAM terms can efficiently be eliminated by unrolling the equations with respect to the number of different modals within the VCI matrix elements. Simple prescreening of the VAM terms cannot compete with this implementation. This allows to consider 0D VAM terms for all VCI matrix elements plus 1D VAM terms for the diagonal terms in standard applications by default, which is of particular relevance for rovibrational calculations requiring high accuracy. The introduction of prediagonalizations in configuration selective VCI algorithms is a subtle technique, which leads to an overall stabilization of the selection process and, at the same time, leads to moderate acceleration of these calculations. Both approaches essentially have no impact on the final results, but increase the efficiency of VCI implementations and thus allow to handle larger correlation spaces or even larger molecules. In the subsequent paper within this series, cf. Reference [39], even further techniques for accelerating VCI calculations will be presented.

DATA AVAILABILITY STATEMENT

The data that support the findings of this study are available from the corresponding author upon reasonable request.

ORCID

Guntram Rauhut https://orcid.org/0000-0003-0623-3254

REFERENCES

[1] K. M. Christoffel, J. M. Bowman, *Chem. Phys. Lett.* **1982**, *85*, 220.
[2] M. Neff, G. Rauhut, *J. Chem. Phys.* **2009**, *131*(12), 124129.
[3] M. Sibaev, D. L. Crittenden, *J. Chem. Phys.* **2016**, *145*(6), 064106.
[4] J. H. Fetherolf, T. C. Berkelbach, *J. Chem. Phys.* **2021**, *154*(7), 074104.
[5] R. Garnier, M. Odunlami, V. L. Bris, D. Begue, I. Baraille, O. Coulaud, *J. Chem. Phys.* **2016**, *144*, 204123.
[6] J. M. Bowman, K. Christoffel, F. Tobin, *J. Phys. Chem.* **1979**, *83*, 905.
[7] S. Carter, J. M. Bowman, N. C. Handy, *Theor. Chem. Acc.* **1998**, *100*, 191.
[8] M. Sibaev, D. L. Crittenden, *Comput. Phys. Commun.* **2016**, *203*, 290.
[9] P. Carbonniere, A. Dargelos, C. Pouchan, *Theor. Chem. Acc.* **2010**, *125*(3–6), 543.
[10] D. M. Benoit, *J. Chem. Phys.* **2006**, *125*(24), 244110.
[11] I. Baraille, C. Larrieu, A. Dargelos, *Chem. Phys.* **2001**, *273*, 91.

[12] M. Odunlami, V. L. Bris, D. Begue, I. Baraille, O. Coulaud, *J. Chem. Phys.* **2017**, *146*, 214108.

[13] N. Gohaud, D. Begue, C. Darrigan, C. Pouchan, *J. Comput. Chem.* **2005**, *26*(7), 743.

[14] T. Petrenko, G. Rauhut, *J. Chem. Phys.* **2017**, *146*(12), 124101.

[15] D. Oschetzki, M. Neff, P. Meier, F. Pfeiffer, G. Rauhut, *Croat. Chem. Acta* **2012**, *85*, 379.

[16] H. J. Werner, P. J. Knowles, F. R. Manby, J. A. Black, K. Doll, A. Heßelmann, D. Kats, A. Köhn, T. Korona, D. A. Kreplin, Q. Ma, T. F. Miller III., A. Mitrushchenkov, K. A. Peterson, I. Polyak, G. Rauhut, M. Sibaev, *J. Chem. Phys.* **2020**, *152*(14), 144107.

[17] J. K. Watson, *Mol. Phys.* **1968**, *15*(5), 479.

[18] S. Carter, J. M. Bowman, L. B. Harding, *Spectrochim. Acta A* **1997**, *53*(8), 1179.

[19] S. Carter, S. J. Culik, J. M. Bowman, *J. Chem. Phys.* **1997**, *107*(24), 10458.

[20] P. T. Panek, C. R. Jacob, *J. Chem. Phys.* **2016**, *144*(16), 164111.

[21] J. O. Jung, R. B. Gerber, *J. Chem. Phys.* **1996**, *105*(23), 10332.

[22] K. Yagi, K. Hirao, T. Taketsugu, M. W. Schmidt, M. S. Gordon, *J. Chem. Phys.* **2004**, *121*(3), 1383.

[23] O. Christiansen, *Phys. Chem. Chem. Phys.* **2007**, *9*, 2942.

[24] P. Carbonniere, V. Barone, *Chem. Phys. Lett.* **2004**, *392*(4), 365.

[25] M. Neff, T. Hrenar, D. Oschetzki, G. Rauhut, *J. Chem. Phys.* **2011**, *134*(6), 064105.

[26] T. Mathea, G. Rauhut, *J. Chem. Phys.* **2020**, *152*(19), 194112.

[27] K. Pflüger, M. Paulus, S. Jagiella, T. Burkert, G. Rauhut, *Theor. Chem. Acc.* **2005**, *114*, 327.

[28] K. Yagi, S. Hirata, K. Hirao, *Theor. Chim. Acta* **2007**, *118*, 681.

[29] M. Sparta, M. B. Hansen, E. Matito, D. Toffoli, O. Christiansen, *J. Chem. Theory Comput.* **2010**, *6*, 3162.

[30] B. Ziegler, G. Rauhut, *J. Phys. Chem. A* **2019**, *123*(15), 3367.

[31] T. Mathea, T. Petrenko, G. Rauhut, *J. Phys. Chem. A* **2021**, *125*(19), 194112.

[32] D. F. Dinu, B. Ziegler, M. Podewitz, et al., *J. Mol. Spectrosc.* **2020**, *367*, 111224.

[33] B. Ziegler, G. Rauhut, *J. Chem. Phys.* **2016**, *144*(11), 114114.

[34] J. M. Bowman, *Acc. Chem. Res.* **1986**, *19*(7), 202.

[35] J. M. Bowman, *J. Chem. Phys.* **1978**, *68*(2), 608.

[36] G. Rauhut, *J. Chem. Phys.* **2004**, *121*(19), 9313.

[37] G. Rauhut, *J. Chem. Phys.* **2007**, *127*(18), 184109.

[38] Y. Scribano, D. M. Benoit, *Chem. Phys. Lett.* **2008**, *458*(4), 384.

[39] T. Mathea, T. Petrenko, G. Rauhut, *J. Comput. Chem.* **2021**. https://doi.org/10.1002/JCC.26764.

SUPPORTING INFORMATION

Additional supporting information may be found in the online version of the article at the publisher's website.

APPENDIX A.

A.1. | Vibrational angular momentum terms of first order

The calculation of the first order vibrational angular momentum (VAM) terms, which may be important for highly accurate rovibrational calculations, is even more demanding than that of the zeroth order elements. For the sake of completeness, we provide the respective working equations for the first order VAM terms in the following. We have split up contributions resulting from different integrals/operators in some of the cases. Note that, within the implementation of all following expressions in our program, we explicitly use Equation (10a), which leads to an additional noticeably reduction of elements within the individual sums, but which is not exploited in the equations below for the purpose of a better readability.

A.2. | Notation

Let $M \neq \emptyset$ be an arbitrary set. Furthermore, let S_M with

$$S_M = \{ f : M \to M | f \text{ bijectiv} \} \tag{A1}$$

be the set of all bijective maps from M to itself, that is, the set of permutations on the set M. $(S_M, \circ)$ forms a group with the composition of mappings being the group operation.

In the following, we use Cauchy's two-line notation in order to denote a permutation $\sigma \in S_M$ with $|M| = m$ and $M = \{i_1, i_2, ... i_m\}$, that is,

$$\sigma = \begin{pmatrix} i_1 & i_2 & ... & i_m \\ \sigma(i_1) & \sigma(i_2) & ... & \sigma(i_m) \end{pmatrix}. \tag{A2}$$

or, shorter,

$$\sigma = \begin{pmatrix} 1 & 2 & ... & m \\ \sigma(1) & \sigma(2) & ... & \sigma(m) \end{pmatrix}. \tag{A3}$$

Furthermore, it applies $|S_M| = m!$ if $m \in \mathbb{N}$.

We further introduce the following sets: As in Section 4, we assume $|\Phi_I\rangle = |\prod_k \varphi_k^{n_k^I}\rangle$ and $|\Phi_J\rangle = |\prod_k \varphi_k^{n_k^J}\rangle$ and $M_m = \{i_1, ..., i_m\}$ being the set of modes which differ by the occupation numbers n_k^I and n_k^J. Let now $M_A = \{k_1, k_2, ..., k_M\}$, $|M_A| = M$ be the set of all available mode indices of a system with M degrees of freedom. Let $M_I = M_A \setminus M_m = \{j_1, ..., j_{M-m}\}$, $|M_I| = M - m$ be the set difference of M_A and M_m. We denote the union of M_m and an arbitrary element $j_k, 1 \leq k \leq M - m$ from the set M_I by

$$\tilde{M}_{m,k} = M_m \cup \{j_k\} \, | \, j_k \in M_I. \tag{A4}$$

$S_{\tilde{M}_{m,k}}$ with $\tilde{\sigma} \in S_{\tilde{M}_{m,k}}$ and $|S_{\tilde{M}_{m,k}}| = (m+1)!$ denotes the set of all bijective self-mappings of $\tilde{M}_{m,k}$. Furthermore, let

$$\tilde{M}_{m,k,l} = \{M_{m,k} \cup \{j_l\} | j_l \in M_I \wedge l \neq k\} \tag{A5}$$

be the union of $M_{m,k}$ and an element $j_l, 1 \leq l \leq M - m$ with $l \neq k$ of the set M_I. The set of all bijective self-mappings of $\tilde{M}_{m,k,l}$ is denoted $S_{\tilde{M}_{m,k,l}}$, $\sigma' \in S_{\tilde{M}_{m,k,l}}$ with $|S_{\tilde{M}_{m,k,l}}| = (m+2)!$.

A.2.1. | Offdiagonal elements with $m = 5$

Let $M_5 = \{i_1, i_2, i_3, i_4, i_5\}$. Due to the orthogonality of the modals, only integrals with five different indices contribute, which solely are of the form $\langle q_r \partial_{q_s} \mu_{\alpha\beta}(q_v) q_t \partial_{q_u} \rangle$. Within this, only the permutations of M_5 yield non-zero terms. Using Cauchy's two-line notation (A3), the matrix elements with $m = 5$ can be written in a compact form as

$$\langle \Phi_I | H_{\text{VAM,1D}}^{(m=5)} | \Phi_J \rangle$$
$$= -\frac{1}{2} \sum_{\alpha\beta} \sum_{\sigma \in S_{M_5}} \zeta^{\alpha}_{\sigma(1)\sigma(2)} \zeta^{\beta}_{\sigma(3)\sigma(4)} \langle \mu_{\alpha\beta}(q_{\sigma(1)}) \rangle \langle q_{\sigma(2)} \rangle \langle \partial_{q_{\sigma(3)}} \rangle \langle q_{\sigma(4)} \rangle \langle \partial_{q_{\sigma(5)}} \rangle, \tag{A6}$$

that is, independent of the number of modes, $6! = 120$ products of integrals have to be summed up instead of $\mathcal{O}(M^5)$.

A.2.2. | Offdiagonal elements with $m = 4$

Let $M_4 = \{i_1, i_2, i_3, i_4\}$. Due to the orthogonality of the modals, integrals having less than four different indices vanish. In the case of integrals with exactly four indices, all permutations of M_4 have to be considered. Non-zero contributions of these are:

Sum of contribution of types $\langle q_r \partial_{q_s} \mu_{\alpha\beta}(q_i) q_t \partial_{q_u} \rangle$ $(i \in \{r, s, t, u\})$, which can be united due to the same prefactor:

$$-\frac{1}{2} \sum_{\alpha\beta} \sum_{\sigma \in S_{M_4}} \zeta^{\alpha}_{\sigma(1)\sigma(2)} \zeta^{\beta}_{\sigma(3)\sigma(4)}$$
$$\left[\langle \partial_{q_{\sigma(2)}} \rangle \langle \partial_{q_{\sigma(4)}} \rangle \left(\langle \mu_{\alpha\beta}(q_{\sigma(1)}) q_{\sigma(1)} \rangle \langle q_{\sigma(3)} \rangle + \langle \mu_{\alpha\beta}(q_{\sigma(3)}) q_{\sigma(3)} \rangle \langle q_{\sigma(1)} \rangle \right) \right.$$
$$\left. + \langle q_{\sigma(1)} \rangle \langle q_{\sigma(3)} \rangle \left(\langle \mu_{\alpha\beta}(q_{\sigma(2)}) \partial_{q_{\sigma(2)}} \rangle \langle \partial_{q_{\sigma(4)}} \rangle + \langle \mu_{\alpha\beta}(q_{\sigma(4)}) \partial_{q_{\sigma(4)}} \rangle \langle \partial_{q_{\sigma(2)}} \rangle \right) \right] \tag{A7}$$

Let $\tilde{S}_{M_4}$ be the subset

$$\tilde{S}_{M_4} = S_{M_4} \setminus \{\sigma \in S_{M_4} | \sigma : \sigma(3) > \sigma(2)\} \tag{A8}$$

with $|\tilde{S}_{M_4}| = 4!/2$. Then it holds for the contribution of $\langle q_r^2 \partial_{q_s} \mu_{\alpha\beta}(q_v) \partial_{q_u} \rangle$

$$-\frac{1}{2} \sum_{\alpha\beta} \sum_{\sigma \in \tilde{S}_{M_4}} \zeta^{\alpha}_{\sigma(1)\sigma(2)} \zeta^{\beta}_{\sigma(1)\sigma(3)} \langle \mu_{\alpha\beta}(q_{\sigma(4)}) \rangle \langle q_{\sigma(1)}^2 \rangle \langle \partial_{q_{\sigma(2)}} \rangle \langle \partial_{q_{\sigma(3)}} \rangle, \tag{A9}$$

since due to the symmetry of the integral regarding interchanging the indices s and u, summation over all α, β, and v not coupling to other indices, only the subset $\tilde{S}_{M_4}$ has to be taken into account.

Let S'_{M_4} be the subset defined as

$$S'_{M_4} = S_{M_4} \setminus \{ \sigma \in S_{M_4} \sigma : \sigma(3) > \sigma(1) \} \quad (A10)$$

with $S'_{M_4} = 4!/2$ The integral $\left\langle q_r \partial^2_{q_s} \mu_{\alpha\beta}(q_v) q_t \right\rangle$ contributes by

$$-\frac{1}{2} \sum_{\alpha\beta} \sum_{\sigma \in S'_{M_4}} \zeta^\alpha_{\sigma(1)\sigma(2)} \zeta^\beta_{\sigma(3)\sigma(2)} \left\langle \mu_{\alpha\beta}\left(q_{\sigma(4)}\right) \right\rangle \left\langle q_{\sigma(1)} \right\rangle \left\langle \partial^2_{q_{\sigma(2)}} \right\rangle \left\langle q_{\sigma(3)} \right\rangle, \quad (A11)$$

obtained via similar considerations as for $\left\langle q^2_r \partial_{q_s} \mu_{\alpha\beta}(q_v) \partial_{q_u} \right\rangle$.

Sum of contributions of types $\left\langle q_r \partial_{q_s} q_s \mu_{\alpha\beta}(q_v) \partial_{q_u} \right\rangle$ and $\left\langle q_r \partial_{q_r} \partial_{q_s} \mu_{\alpha\beta}(q_v) q_t \right\rangle$, which can be combined due to Equation (11):

$$-\frac{1}{2} \sum_{\alpha\beta} \sum_{\sigma \in S_{M_4}} \left(\zeta^\alpha_{\sigma(1)\sigma(2)} \zeta^\beta_{\sigma(2)\sigma(3)} + \zeta^\alpha_{\sigma(2)\sigma(3)} \zeta^\beta_{\sigma(1)\sigma(2)} \right) \left\langle \mu_{\alpha\beta}\left(q_{\sigma(4)}\right) \right\rangle \left\langle q_{\sigma(1)} \right\rangle \left\langle \partial_{q_{\sigma(2)}} q_{\sigma(2)} \right\rangle \left\langle \partial q_{\sigma(3)} \right\rangle$$

$$(A12)$$

There is one integral having five different indices. In this case, all permutations of M_4 have to be considered, while there is one free index I having $M - m$ possible values. Therefore, the contribution of $\left\langle q_s \partial_{q_s} \mu_{\alpha\beta}(q_v) q_t \partial_{q_u} \right\rangle$ yields

$$-\frac{1}{2} \sum_{\alpha\beta} \sum_{k=1}^{M-m} \sum_{\tilde\sigma \in S_{\tilde M_{4,k}}} \left[\zeta^\alpha_{\tilde\sigma(1)\tilde\sigma(2)} \zeta^\beta_{\tilde\sigma(3)\tilde\sigma(4)} \left\langle \mu_{\alpha\beta}\left(q_{\tilde\sigma(5)}\right) \right\rangle \left\langle q_{\tilde\sigma(1)} \right\rangle \left\langle \partial_{q_{\tilde\sigma(2)}} \right\rangle \left\langle q_{\tilde\sigma(3)} \right\rangle \left\langle \partial_{q_{\tilde\sigma(4)}} \right\rangle \right]$$

$$(A13)$$

The matrix element $\left\langle \Phi_I | | H^{(m=4)}_{\text{VAM,1D}} | \Phi_J \right\rangle$ is given as the sum of the expressions (A7), (A9), (A11), (A12), and (A13).

A.2.3. | Offdiagonal elements with $m = 3$

In the case of integrals having three different indices, solely the elements of S_{M_3} have to be taken into account for possible index combinations, that is, $3! = 6$ combinations are remaining. Terms having the same prefactors can be grouped as follows:

Sum of contributions of types $\left\langle q_r \partial_{q_s} \mu_{\alpha\beta}(q_i) q_r \partial_{q_u} \right\rangle, i \in \{r,s,u\}$ and $\left\langle q_r \partial_{q_s} \mu_{\alpha\beta}(q_j) q_t \partial_{q_u} \right\rangle, j \in \{r,s,t\}$:

$$-\frac{1}{2} \sum_{\alpha\beta} \sum_{\sigma \in S_{M_3}} \zeta^\alpha_{\sigma(1)\sigma(2)} \zeta^\beta_{\sigma(1)\sigma(3)}$$

$$\left[\left\langle \partial_{q_{\sigma(2)}} \right\rangle \left(\left\langle \mu_{\alpha\beta}(q_{\sigma(1)}) q^2_{\sigma(1)} \right\rangle \left\langle \partial_{q_{\sigma(3)}} \right\rangle + \left\langle \mu_{\alpha\beta}(q_{\sigma(3)}) \partial_{q_{\sigma(3)}} \right\rangle \left\langle q^2_{\sigma(1)} \right\rangle - \left\langle \mu_{\alpha\beta}(q_{\sigma(1)}) q_{\sigma(1)} \partial_{q_{\sigma(1)}} \right\rangle \left\langle q_{\sigma(3)} \right\rangle \right.$$

$$\left. - \left\langle \mu_{\alpha\beta}(q_{\sigma(3)}) q_{\sigma(3)} \right\rangle \left\langle q_{\sigma(1)} \partial_{q_{\sigma(1)}} \right\rangle \left\langle \partial_{q_{\sigma(3)}} \right\rangle \right) + \left\langle \mu_{\alpha\beta}(q_{\sigma(2)}) \partial_{q_{\sigma(2)}} \right\rangle \left(\left\langle q^2_{\sigma(1)} \right\rangle \left\langle \partial_{q_{\sigma(3)}} \right\rangle - \left\langle q_{\sigma(1)} \partial_{q_{\sigma(1)}} \right\rangle \left\langle q_{\sigma(3)} \right\rangle \right) \right]$$

$$(A14)$$

Sum of contributions of $\left\langle q_r \partial_{q_s} \mu_{\alpha\beta}(q_i) q_s \partial_{q_u} \right\rangle, i \in \{r,s,u\}$ and $\left\langle q_r \partial_{q_s} \mu_{\alpha\beta}(q_j) q_t \partial_{q_s} \right\rangle, j \in \{r,s,t\}$:

$$-\frac{1}{2} \sum_{\alpha\beta} \sum_{\sigma \in S_{M_3}} \zeta^\alpha_{\sigma(1)\sigma(2)} \zeta^\beta_{\sigma(2)\sigma(3)}$$

$$\left[\left\langle q_{\sigma(1)} \right\rangle \left(\left\langle \mu_{\alpha\beta}(q_{\sigma(2)}) \partial_{q_{\sigma(2)}} q_{\sigma(2)} \right\rangle \left\langle \partial_{q_{\sigma(3)}} \right\rangle + \left\langle \mu_{\alpha\beta}(q_{\sigma(3)}) \partial_{q_{\sigma(3)}} \right\rangle \left\langle \partial_{q_{\sigma(2)}} q_{\sigma(2)} \right\rangle - \left\langle \mu_{\alpha\beta}(q_{\sigma(2)}) \partial^2_{q_{\sigma(2)}} \right\rangle \left\langle q_{\sigma(3)} \right\rangle \right.$$

$$\left. - \left\langle \mu_{\alpha\beta}(q_{\sigma(3)}) q_{\sigma(3)} \partial^2_{q_{\sigma(2)}} \right\rangle \right) + \left\langle \mu_{\alpha\beta}(q_{\sigma(1)}) q_{\sigma(1)} \right\rangle \left(\left\langle \partial_{q_{\sigma(2)}} q_{\sigma(2)} \right\rangle \left\langle \partial_{q_{\sigma(3)}} \right\rangle - \left\langle \partial^2_{q_{\sigma(2)}} \right\rangle \left\langle q_{\sigma(3)} \right\rangle \right) \right]$$

$$(A15)$$

Sum of contributions of $\left\langle q_r \partial_{q_s} \mu_{\alpha\beta}(q_v) q_s \partial_{q_r} \right\rangle$ and $\left\langle q_r \partial_{q_s} \mu_{\alpha\beta}(q_v) q_r \partial_{q_s} \right\rangle$:

$$-\frac{1}{2} \sum_{\alpha\beta} \sum_{\sigma \in S_{M_3}} \zeta^\alpha_{\sigma(1)\sigma(2)} \zeta^\beta_{\sigma(1)\sigma(2)} \left\langle \mu_{\alpha\beta}\left(q_{\sigma(3)}\right) \right\rangle$$

$$\left[\left\langle q_{\sigma(1)} \partial_{\sigma(1)} \right\rangle \left\langle \partial_{\sigma(2)} q_{\sigma(2)} \right\rangle - \left\langle q^2_{\sigma(1)} \right\rangle \left\langle q^2_{\sigma(2)} \right\rangle \right]$$

$$(A16)$$

For integrals having four different indices there is one free index left after considering elements of S_{M_3}. By using Equation (A4), the non-zero contributions are the following:

Sum of contributions of types $\left\langle q_r \partial_{q_s} \mu_{\alpha\beta}(q_i) q_t \partial_{q_u} \right\rangle, i \in \{r,s,t,u\}$:

$$-\frac{1}{2} \sum_{\alpha\beta} \sum_{k=1}^{M-m} \sum_{\tilde\sigma \in S_{\tilde M_{3,k}}} \zeta^\alpha_{\tilde\sigma(1)\tilde\sigma(2)} \zeta^\beta_{\tilde\sigma(3)\tilde\sigma(4)}$$

$$\left[\left\langle \partial_{q_{\tilde\sigma(2)}} \right\rangle \left\langle \partial_{q_{\tilde\sigma(4)}} \right\rangle \left(\left\langle \mu_{\alpha\beta}(q_{\tilde\sigma(1)}) q_{\tilde\sigma(1)} \right\rangle \left\langle q_{\tilde\sigma(3)} \right\rangle + \left\langle \mu_{\alpha\beta}(q_{\tilde\sigma(3)}) q_{\tilde\sigma(3)} \right\rangle \left\langle q_{\tilde\sigma(1)} \right\rangle \right) \right.$$

$$\left. + \left\langle q_{\tilde\sigma(1)} \right\rangle \left\langle q_{\tilde\sigma(3)} \right\rangle \left(\left\langle \mu_{\alpha\beta}(q_{\tilde\sigma(2)}) \partial_{q_{\tilde\sigma(2)}} \right\rangle \left\langle \partial_{q_{\tilde\sigma(4)}} \right\rangle + \left\langle \mu_{\alpha\beta}(q_{\tilde\sigma(4)}) \partial_{q_{\tilde\sigma(4)}} \right\rangle \left\langle \partial_{q_{\tilde\sigma(2)}} \right\rangle \right) \right]$$

$$(A17)$$

Sum of contributions of types $\left\langle q_r \partial_{q_s} \mu_{\alpha\beta}(q_v) q_t \partial_{q_i} \right\rangle, i \in \{r,s\}$ and $\left\langle q_r \partial_{q_s} \mu_{\alpha\beta}(q_v) q_j \partial_{q_u} \right\rangle, j \in \{r,s\}$:

$$-\frac{1}{2} \sum_{\alpha\beta} \sum_{k=1}^{M-m} \sum_{\tilde\sigma \in S_{M_{3,k}}} \zeta^\alpha_{\tilde\sigma(1)\tilde\sigma(2)} \left\langle \mu_{\alpha\beta}\left(q_{\tilde\sigma(4)}\right) \right\rangle$$

$$\left[\left\langle q_{\tilde\sigma(3)} \right\rangle \left(\zeta^\beta_{\tilde\sigma(3)\tilde\sigma(2)} \left\langle q_{\tilde\sigma(1)} \right\rangle \left\langle \partial^2_{q_{\tilde\sigma(2)}} \right\rangle + \zeta^\beta_{\tilde\sigma(3)\tilde\sigma(1)} \left\langle q_{\tilde\sigma(1)} \partial_{q_{\tilde\sigma(1)}} \right\rangle \left\langle \partial_{q_{\tilde\sigma(2)}} \right\rangle \right) \right.$$

$$\left. + \left\langle \partial_{q_{\tilde\sigma(3)}} \right\rangle \left(\zeta^\beta_{\tilde\sigma(2)\tilde\sigma(3)} \left\langle q_{\tilde\sigma(1)} \right\rangle \left\langle \partial_{q_{\tilde\sigma(2)}} q_{\tilde\sigma(2)} \right\rangle + \zeta^\beta_{\tilde\sigma(1)\tilde\sigma(3)} \left\langle q^2_{\tilde\sigma(1)} \partial_{q_{\tilde\sigma(1)}} \right\rangle \left\langle \partial_{q_{\tilde\sigma(2)}} \right\rangle \right) \right]$$

$$(A18)$$

Within the only integral having five different indices, $\left\langle q_r \partial_{q_s} \mu_{\alpha\beta}(q_v) q_t \partial_{q_u} \right\rangle$, the set M_3 fixes three of them. Thus, for the two indices left all modes being not in M_3 have to combined with those in M_3. Using Equation (A5), one obtains for the contribution of $\left\langle q_r \partial_{q_s} \mu_{\alpha\beta}(q_v) q_t \partial_{q_u} \right\rangle$:

$$-\frac{1}{2} \sum_{\alpha\beta} \sum_{k=1}^{M-m} \sum_{l=1}^{M-m-1} \sum_{\sigma' \in S_{\tilde M_{3,kl}}} \zeta^\alpha_{\sigma'(1)\sigma'(2)} \zeta^\beta_{\sigma'(3)\sigma'(4)}$$

$$\left\langle \mu_{\alpha\beta}\left(q_{\sigma'(5)}\right) \right\rangle \left\langle q_{\sigma'(1)} \right\rangle \left\langle \partial_{q_{\sigma'(2)}} \right\rangle \left\langle q_{\sigma'(3)} \right\rangle \left\langle \partial_{q_{\sigma'(4)}} \right\rangle$$

$$(A19)$$

The matrix element $\left\langle \Phi_I | H^{(m=3)}_{\text{VAM,1D}} | \Phi_J \right\rangle$ is given as sum of the expressions (A14), (A15), (A16), (A17), (A18), and (A19).

A.2.4. | Offdiagonal elements with $m = 2$ and $m = 1$

Since there are no considerable simplifications leading to large computational saving for these two cases, we neglect these.

A.3. | Diagonal elements

All integrals containing the term $\langle \partial_{q_i} \rangle$ vanish due to Equation (10a). The non-vanishing contributions are the following:

Contributions of integrals with only two different indices:

$$-\frac{1}{2}\sum_{\alpha\beta}\sum_{s}\sum_{r<s}\zeta_{rs}^{\alpha}\zeta_{sr}^{\beta}$$

$$\left[\frac{1}{2}\langle\mu_{\alpha\beta}(q_r)q_r\partial_{q_r}\rangle+\frac{1}{2}\langle\mu_{\alpha\beta}(q_s)q_s\partial_{q_s}\rangle-\frac{1}{2}\langle\mu_{\alpha\beta}(q_r)\partial_{q_r}q_r\rangle-\frac{1}{2}\langle\mu_{\alpha\beta}(q_s)\partial_{q_s}q_s\rangle\right.$$

$$-\langle\mu_{\alpha\beta}(q_r)q_r^2\rangle\langle\partial_{q_s}^2\rangle-\langle\mu_{\alpha\beta}(q_s)q_s^2\rangle\langle\partial_{q_r}^2\rangle$$

$$\left.-\langle\mu_{\alpha\beta}(q_s)\partial_{q_s}^2\rangle\langle q_r^2\rangle-\langle\mu_{\alpha\beta}(q_r)\partial_{q_r}^2\rangle\langle q_s^2\rangle\right]$$

$$\tag{A20}$$

Contributions of integrals with only three different indices:

$$-\frac{1}{2}\sum_{\alpha\beta}\sum_{rst}\left[\frac{1}{2}\left(-\zeta_{rs}^{\alpha}\zeta_{tr}^{\beta}+\zeta_{tr}^{\alpha}\zeta_{rs}^{\beta}\right)\langle\mu_{\alpha\beta}(q_s)\partial_{q_s}\rangle\langle q_t\rangle\right.$$

$$+\left(\zeta_{rs}^{\alpha}\zeta_{ts}^{\beta}+\zeta_{ts}^{\alpha}\zeta_{rs}^{\beta}\right)\langle\mu_{\alpha\beta}(q_r)q_r\rangle\langle q_t\rangle\langle\partial_{q_s}^2\rangle$$

$$+\zeta_{rs}^{\alpha}\zeta_{ts}^{\beta}\langle\mu_{\alpha\beta}(q_s)\partial_{q_s}^2\rangle\langle q_r\rangle\langle q_t.\rangle+\zeta_{rs}^{\alpha}\zeta_{rs}^{\beta}\langle\mu_{\alpha\beta}(q_t)\rangle\left(\frac{1}{4}+\langle q_r^2\rangle\langle\partial_{q_s}^2\rangle\right)\right]$$

$$\tag{A21}$$

Contribution of $\langle q_r\partial_{q_s}^2\mu_{\alpha\beta}(q_v)q_t\rangle$:

$$-\frac{1}{2}\sum_{\alpha\beta}\sum_{vrst}\zeta_{rs}^{\alpha}\zeta_{ts}^{\beta}\langle\mu_{\alpha\beta}(q_v)\rangle\langle q_r\rangle\langle\partial_{q_s}^2\rangle\langle q_t\rangle\tag{A22}$$

$\langle\Phi_I|H_{VAM,1D}^{(m=0)}|\Phi_I\rangle$ is given by the sum of the expressions (A20), (A21), and (A22).